https://doi.org/10.5194/egusphere-2026-2701
Preprint. Discussion started: 22 May 2026

Convective activity within a tropical cyclone undergoing extratropical transition over a warmer ocean.

Pedro Gómez-Plasencia[1], Ernesto Javier Rodríguez-Acosta[1], Juan Jesús González-Alemán[2], Carlos Calvo-Sancho[3], Pedro Bolgiani[4], Javier Díaz-Fernández[1,2], Ana Montoro-Mendoza[1,2], María Luisa Martín[1], Íñigo Gómara[1]

[1]Department of Applied Mathematics, School of Computer Engineering (SG), University of Valladolid, Segovia, Spain.
[2]State Meteorological Agency (AEMET), Madrid, Spain.
[3]Center for Desertification Research, Spanish National Research Council (CIDE, CSIC-UV-GVA), Climate, Atmosphere and Ocean Laboratory (Climatoc-Lab), Moncada, Valencia, Spain.
[4]Department of Earth Physics and Astrophysics, Faculty of Physical Sciences, Complutense University of Madrid, Madrid, Spain.

Correspondence to: Pedro Gómez-Plasencia (pedrogp@uva.es)

Abstract. The Northeastern Atlantic basin is a region where the number of cyclones with tropical features can increase in the future due to anthropogenic climate change, a particularly important concern given the region's vulnerability to such systems. This work analyses the influence of warmer sea surface temperatures (SSTs), expected in future climates, in the convective activity of Tropical Storm Delta. Delta, which caused strong damage over the Canary Islands (Spain) in November 2005, is representative of a tropical cyclone (TC) experiencing an extratropical transition (ET) on its path to western Europe. Two simulations of the storm were performed with the high-resolution atmospheric numerical model HARMONIE-AROME: a control simulation with initial and boundary conditions from the ERA5 reanalysis, and a warm simulation where a uniform perturbation of +2 ºC was added to the SSTs surrounding the cyclone. The convective activity was analysed only in the convective cells near the cyclone's centre, employing the cloud tracking package Tobac, based on brightness temperature. Results show that increases in low-level water vapor flux, together with lower LCL and LFC levels and increased CAPE, create an environment more favourable for the development of deep moist convection in the warmer ocean simulation. These thermodynamic changes lead to more frequent intense moist updrafts and a larger number of convective cells associated with the cyclone, with greater vertical extent and higher precipitation rates. Consequently, Delta becomes a more intense and deeper TC, driven by latent heat release, reaching hurricane status. Later, Delta's ET starts earlier and gets extended over time, while turning notably more severe too. These results may contribute to a better understanding of the behaviour of convection within cyclones with tropical characteristics affecting the Macaronesia and Western Europe under future climates.

https://doi.org/10.5194/egusphere-2026-2701
Preprint. Discussion started: 22 May 2026

1 Introduction

The future projections for tropical cyclone (TC) dynamics have been a topic of extended discussion in recent years. The total number of TCs formed is projected to be reduced in future scenarios affected by anthropogenic climate change (ACC), although the frequency of those with high intensity (CAT. 3-5) is expected to increase (Camargo et al., 2023; Garin et al., 2025; Yamada et al., 2017; Zhao et al., 2026). However, these projections for the TC frequency remain subject to considerable uncertainty within the scientific community, while there is a greater consensus on the projected increase in the intensity of TCs (Camargo et al., 2023; Holland & Bruyère, 2014; Yamada et al., 2017). Moreover, the uncertainties increase when these projections are realized on individual basins (Camargo et al., 2023; Roberts et al., 2020). Even though no complete agreement has been reached for the TC frequency, some authors predict a growth in the number of TCs formed and their intensity in the Northeastern Atlantic basin (Emanuel, 2021; Lima et al., 2021; Murakami & Wang, 2010; Oouchi et al., 2006; Sugi et al., 2002; Villarini & Vecchi, 2013).

The evolution of the environments is also quite relevant, since TCs are extremely sensitive to changes in their surroundings (Riehl, 1954; The COMET Program, 2009). In a future warmer climate, sea surface temperatures (SSTs) and atmospheric moisture are expected to increase (Collins et al., 2013; Garcia-Soto et al., 2021; IPCC, 2023). Such changes may significantly affect regions historically devoid of TCs, as they could develop conditions favourable for the survival of a previously formed TC approaching the area (Haarsma et al., 2013). Therefore, western Europe could be a region that may encounter a higher number of low-pressure systems with tropical features during the up-and-coming years (Baatsen et al., 2015; Dekker et al., 2018; Haarsma et al., 2013; Montoro-Mendoza et al., 2026). In fact, in the last decade, several cyclones with tropical origin, such as Ophelia (2017), Leslie (2018), Lorenzo (2019) and Hermine (2022) hit different European nations with important human and socioeconomic impacts in the affected areas (Pasch & Roberts, 2018; Reinhart, 2023; Stewart, 2017; Zelinsky, 2019). A better understanding of these systems is crucial for this region, as it remains poorly prepared and better adaptation strategies are needed.

Tropical Storm Delta (2005) was particularly relevant for the western European region, due to the significant damage to infrastructure it produced in the Canary Islands (Spain) in November 2005, mainly due to its associated wind gusts (Beven, 2006; Martín León et al., 2005), after completing its Extratropical Transition (ET; Evans et al., 2017). Before initiating its ET, Delta experienced a tropical phase in which convection was the primary mechanism sustaining the system. These convective processes are strongly dependent on the thermodynamical environment, relying on the availability of warm and moist air at low levels (Markowski & Richardson, 2010). Warm SSTs act as the primary source of that heat and moisture that fuels deep convection, playing a key role for TCs (Dare & McBride, 2011). Future warmer climates are projected to favour the conditions for the development of convective systems (Lepore et al., 2021), as increasing oceanic and atmospheric temperatures will enhance the low-level moisture content and the atmospheric instability, increasing the convective updrafts and the latent heat release (Fischer & Knutti, 2015; Fowler et al., 2021). Within a TC, these changes may lead to a more efficient diabatic heating of its core, a more organized eyewall, and a reinforcement of the system. Therefore, increases in

https://doi.org/10.5194/egusphere-2026-2701
Preprint. Discussion started: 22 May 2026

SSTs driven by ACC could significantly influence the organization, intensity, and extent of the cyclone's convective activity, with direct implications for the system's strength and lifetime.

This study aims to broaden the current understanding of the thermodynamics within TCs experiencing the ET, under future climate scenarios driven by ACC, in a specific case of a cyclone affecting western Europe. Specifically, the main goal is to analyse the sensitivity of the convective activity within Tropical Storm Delta and its behaviour for a 2 ºC increase in the surrounding SSTs. The +2 ºC perturbation represents projected increases in North Atlantic November SSTs relative to 2005, extrapolated from the trend observed over the past 30 years. These projections suggest that such warming could be reached by the end of the XXI century, although this refers to climatological averages, and isolated seasonal anomalies of +2 ºC may occur earlier during the second half of the century in individual years due to internal variability (Fig. S1 of the supplementary material). This is consistent with CMIP6 model simulations (Eyring et al., 2016), which project that increase in the SSTs during the latter half of the century under high-emission scenarios (SSP5-8.5), and by the end of the century under moderate scenarios (SSP2-4.5, SSP3-7.0; IPCC, 2023).

The paper is organized as follows: in Sect. 2 the model and the simulations are described, with the data and the methodology employed for the analysis to be realized. Results and discussion are presented in Sect. 3, where Sect. 3.1 introduces the case study and Sect. 3.2 analyses the numerical simulations. Finally, a summary and the main conclusions are included in Sect. 4.

2 Data and Methodology

2.1 Data

This sensitivity experiment to SST is carried out using the convection-permitting HARMONIE-AROME model cy43h1 (Bengtsson et al., 2017; Calvo-Sancho et al., 2023). HARMONIE-AROME is a spectral, non-hydrostatic, semi-Lagrangian and semi-implicit model. Microscale processes are solved by parameterizations: shallow convection, planetary boundary layer, microphysics, turbulence, radiation, and surface processes (Bengtsson et al., 2017). HARMONIE-AROME allows simulations on a single limited area domain. These have been performed with 2.5 km horizontal resolution, at 65 vertical levels (hybrid sigma pressure coordinates) and a time step of 30 s. Although this model is mainly used for the operational prediction by different national weather services across Europe, it has also been utilized for research purposes, to simulate specific meteorological phenomena, including TCs (Calvo-Sancho et al., 2023; Díaz-Fernández et al., 2022; Quitián-Hernández et al., 2021).

Two different simulations for the Tropical Storm Delta are performed: a control simulation (CSIM) and a +2 ºC simulation (+2SIM). Both cover a period of 97 h, from 26 November 00:00 UTC to 30 November 2005 00:00 UTC. The domain is [12º-35º N, 48º-8º W], centred in the Northeastern Atlantic. The difference between the two simulations is a +2 ºC SST perturbation added to the initial and boundary conditions in the abovementioned domain. Modifying only the SSTs while keeping the atmospheric conditions unchanged follows an approach similar to Rios-Berrios et al. (2024), allowing to isolate the impact of the oceanic warming expected under ACC on tropical convection and precipitation. CSIM is driven by initial

https://doi.org/10.5194/egusphere-2026-2701
Preprint. Discussion started: 22 May 2026

and boundary conditions from ERA5 reanalysis with 0.25º horizontal resolution, 137 hybrid vertical levels and 1-h temporal resolution (Hersbach et al., 2023). Delta's synoptic analysis is also performed using ERA5 data, while the North Atlantic SST trend is analysed using the HadISST database (Rayner et al., 2003).

The Hurricane Database (HURDAT2; Landsea & Franklin, 2013) from the National Hurricane Center (NHC) is used to compare the results from CSIM with the observational data from the best track for Tropical Storm Delta. The NHC uses 1 min averaged wind speeds for their observations (Landsea & Franklin, 2013), while the outputs from HARMONIE-AROME are 10 min averaged wind speeds (Dirksen et al., 2022). Thus, HURDAT wind speeds are multiplied by 0.88, which is the approximated value utilized to transform 1 min to 10 min averaged wind speeds (Sampson et al., 1995), to compare sustained wind speeds from both sources.

2.2 Methodology

Tropical Storm Delta cyclone tracking is performed considering hourly mean sea level pressure (SLP), after applying a Gaussian filter with σ=5 to smooth the small-scale perturbations related to deep moist convection. Then, Delta's position is defined as the location of the minimum filtered mean SLP inside a 5º x 5º box. In the first timestep this box is centred on the cyclone's position according to the report by the NHC (Beven, 2006), while for the following it is centred on the estimated position based on the previous step (Stanković et al., 2024; Wernli & Schwierz, 2006). This process avoids the influence of other synoptical systems that could appear in the complete domain in the simulated period. Basic quantities, such as minimum SLP, maximum 10 m sustained wind speed (sustW10) or maximum 10 m wind gusts, are derived only from values within such box.

The Cyclone Phase Space (CPS; Hart, 2003) is employed to assess the evolution of Tropical Storm Delta's thermodynamic features in both simulations. CPS is a widely used technique to analyse the cyclone lifecycle and the evolution of their structure to classify them in the spectrum between pure tropical and extratropical cyclones (Dekker et al., 2018; González-Alemán et al., 2015; Ribberink et al., 2026). CPS is based on three parameters: thermal asymmetry (B), and thermal wind in the upper (V_T^U; 600-300 hPa) and lower (V_T^L; 900-600 hPa) troposphere. All these parameters are derived from the geopotential height at different levels. The CPS diagrams are smoothed with running means in 12 h windows.

The variables used to characterize convective activity (Table 1) are evaluated only in the cells in the vicinity of the cyclone's centre for both simulations. Herein, the Tracking and Object-Based Analysis of Clouds (Tobac; Allan et al., 2021; Heikenfeld et al., 2019; Sokolowsky et al., 2024) package is employed to track Delta's convective cells, from the brightness temperature (BT) field. Tobac is commonly used to identify and track clouds with different research purposes (Leung et al., 2023), although, to the knowledge of the authors, it has not been used beforehand to track the convective cells within a TC. Tobac's workflow is divided in three steps: the feature identification, the segmentation, and the trajectory linking. First, contiguous regions with BT values below given thresholds (aka features), are identified and labelled. Second, the spatial extension and shape of each feature is calculated through watershedding techniques (segmentation). Finally, the features are

https://doi.org/10.5194/egusphere-2026-2701
Preprint. Discussion started: 22 May 2026

associated with others from different time steps to define the path and evolution of the convective cells to which they belong (trajectory linking).

Table 1: List of variables characterizing convection in HARMONIE-AROME simulations.

Acronym	Name	Units
CT	Cloud Top	m
TP	1-hour Total Precipitation	mm h^{-1}
BT	Brightness Temperature	K
Refl	Reflectivity	dBZ
LCL	Lifting Condensation Level	m
LFC	Level of Free Convection	m
wq	Vertical Transport of Moisture (at 700 hPa)	m s^{-1}
CAPE	Convective Available Potential Energy	J kg^{-1}
WVFlux	Water Vapor Flux (at 925 hPa)	m s^{-1}

Once all the convective cells are detected and located, only those directly related to Delta's convective activity, -i.e., those whose weighted mean centre is located less than 250 km from the filtered SLP minimum-, are considered. Moreover, the convective initiation (CI) is analysed by considering only cells that exceed 35 dBZ reflectivity at any point within their domain (Henderson et al., 2021).

The selection of the thresholds used during the feature identification is of paramount importance. If a too high value of BT is chosen (too permissive), some regions belonging to non-convective clouds (e.g., cirrus) may introduce undesired noise. If the external threshold is excessively restrictive, relevant information from regions with convective activity may be disregarded. Another important parameter is the distance between all the internal thresholds in the BT or step. Tobac identifies an initial volume of cells with BT below the external threshold, and these cells are progressively subdivided as colder thresholds are exceeded. Thus, the step can be understood as a "resolution" in the analysis: if it is too large, it may produce fewer and overly large cells, while if it is too small it can cause excessive cell fragmentation, potentially leading to algorithm errors during the trajectory linking.

This work explores a set of four external BT thresholds (250, 240, 230 and 220 K) and four step sizes (25, 20, 15 and 10 K). The analysis focuses on a configuration with a 220 K external threshold and a 15 K step size, which is considered as the optimal setup after several sensitivity tests with consistent results. This choice minimizes the inclusion of non-convective regions within the cloud bulk and prevents excessive segmentation of the cells, while maintaining a sufficiently fine resolution. In addition, the exploration of all 16 threshold-step combinations provides a robust framework, allowing the consistency of the results to be assessed across a wide range of configurations and reducing methodological uncertainty.

https://doi.org/10.5194/egusphere-2026-2701
Preprint. Discussion started: 22 May 2026

For all the CI features belonging to convective cells associated with Delta and detected by Tobac, values of the fields in Table 1 are recorded in all their grid points. Probability density functions (PDF) of those quantities relevant for convection are represented, and the Mann-Whitney U test (Mann & Whitney, 1947) and the Fisher F-test (Bisgaard & Vardeman, 1995) are applied to assess differences in the mean and variance of distributions from the two simulations (95% confidence interval). Given that the analysis includes all grid points within all the selected convective cells, the resulting distributions are based on a large sample size. This increases the statistical robustness of the results and ensures that the inferred differences are representative of the convective behaviour rather than sampling variability.

3 Results and Discussion

3.1 Tropical Storm Delta

Delta developed out of the region where TCs are usually formed in the Atlantic Ocean as a non-tropical baroclinic low on 19 November 2005, located on 27º N and 48º W (Beven, 2006). It initially displaced towards the northeast and later its trajectory changed to a southward direction (Fig 1a), which was not correctly predicted by Delta's early forecasts (Beven, 2006). On its way to the south, Delta encountered warmer SSTs (24-25 ºC) and low vertical wind shear, which favoured Delta's convection and the formation of a warm core (Da Costa Têso, 2006). Following that, by 23 November, Delta completed the Tropical Transition (TT; Davis & Bosart, 2004; Wood et al., 2023), thus acquiring a warm core driven by convection and a symmetrical horizontal structure. It was then classified by the NHC as a tropical storm, due to its 93 km h^{-1} sustained wind speeds (The Saffir-Simpson Team et al., 2012).

Tropical Storm Delta continued its erratic path towards the south-southeast during a total of 3 days. Delta's peak maximum intensity was recorded on 24 November (Fig. 1b), with 111 km h^{-1} sustained wind speeds and a 980 hPa minimum SLP (Beven, 2006). After this peak Delta started to weaken due to a higher vertical wind shear environment.

On 26 November Delta changed its trajectory towards the northeast and accelerated, strongly influenced by the presence of an upper-level trough (Fig. 1c). On its way to the northeast Delta faced a baroclinic environment, combined with lower SSTs and greater vertical wind shear associated with the midlatitudes. Moreover, a Mesoscale Tropopause Depression (MTD; Browning et al., 2000) caused an intrusion of dry air reaching low tropospheric levels to the southwest of Delta, which restricted the convection to the north-northeast-east sector of the cyclone (Martín León et al., 2005), developing thus an asymmetric convective structure. All these conditions provoked the start of Delta's ET, which was fully completed by 28 November 12:00 UTC (Beven, 2006), deriving in a cold core asymmetric extratropical cyclone.

Later, on the same day, the impacts by Delta over the Canary Islands (Spain) and Madeira (Portugal) were produced, as the centre of the cyclone passed between both archipelagos. In Madeira, located north of the path of the cyclone, where the convection was placed, the main impact was the precipitation, reaching 127 mm in Santo da Serra (660 m.a.s.l.) in 24 h (Da Costa Têso, 2006). The Canary Islands were primarily affected by the very strong wind speeds south of Delta, produced by the interaction between the cyclone and the dry intrusion generated by the MTD, developing a western mesoscale jet-streak

https://doi.org/10.5194/egusphere-2026-2701
Preprint. Discussion started: 22 May 2026

(Martín León et al., 2005). Moreover, the orography of the Canary Islands was also relevant for the strong wind gusts that took place (Martín León et al., 2005), reaching 170 km h^{-1} in Güímar and 248 km h^{-1} in Izaña (2370 m.a.s.l.), resulting on seven casualties and extensive damage to infrastructure and power lines on several islands, among others (Parlamento de Canarias, 2006).

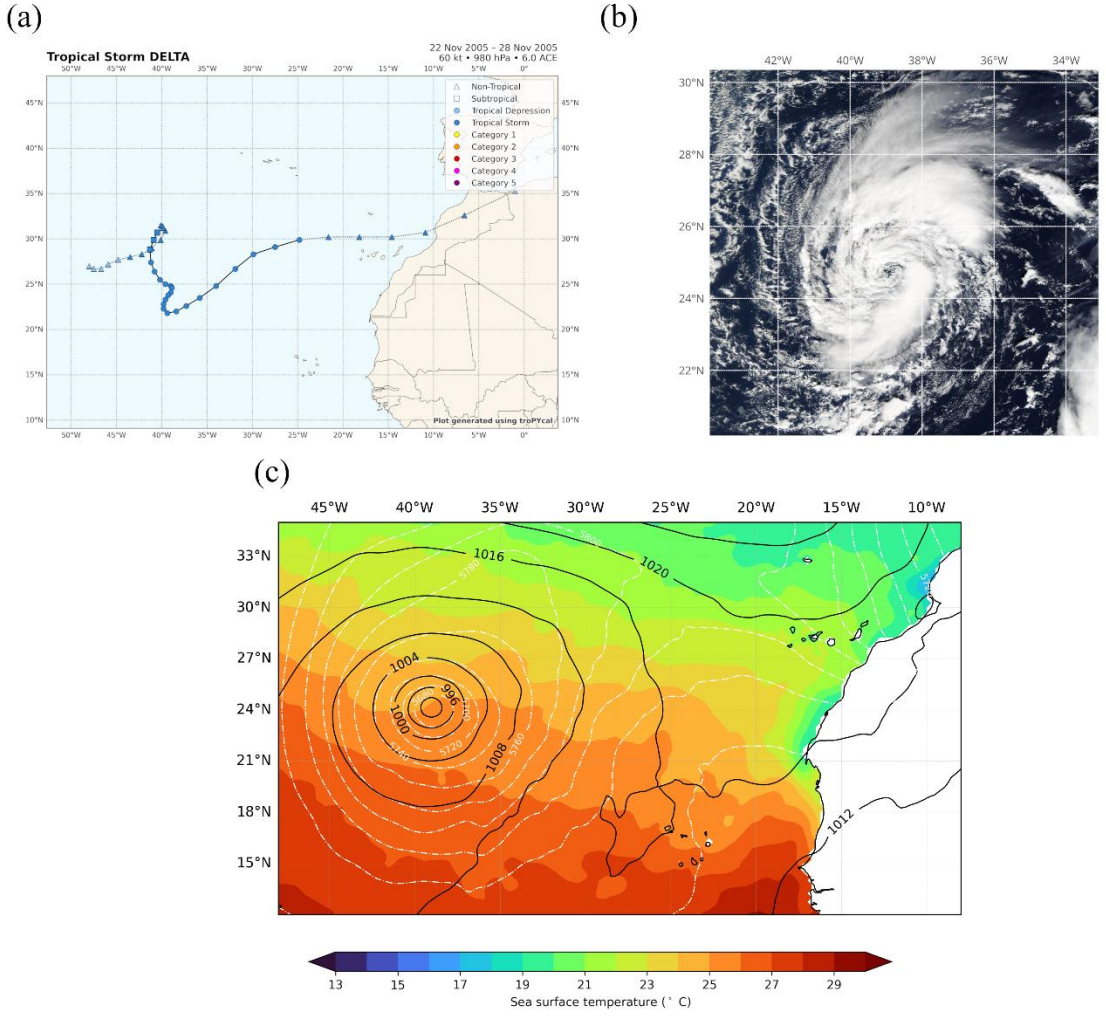

Figure 1: (a) Delta's trajectory from the best track from HURDAT; (b) Delta's image (TERRA / MODIS Corrected Reflectance imagery) at 24 November 2005 00:00 UTC, obtained from Nasa Worldview; (c) Initial synoptic situation for the mean SLP (black contours; hPa), SST (coloured; ºC) and the 500 hPa geopotential height (white dashed contours; m) on 25 November 00:00 UTC from ERA5, utilized as initial conditions for CSIM, in the HARMONIE-AROME domain.

3.2 Numerical Simulations

3.2.1 General Features and Cyclone Phase Space

Figure 2 shows the trajectory and evolution of minimum SLP and maximum sustW10 in CSIM and +2SIM. There is a modest bias between the path in CSIM and the best track from HURDAT in the first hours of the simulation (Fig. 2a),

https://doi.org/10.5194/egusphere-2026-2701
Preprint. Discussion started: 22 May 2026

reducing it in the following hours. Ironically enough, +2SIM appears to match better with the best track from HURDAT. Calvo-Sancho et al. (2023) also noted this lack of agreement between their control-best tracks when reproducing the cyclone's trajectory using HARMONIE-AROME. Here, the trajectory of the cyclone is shifted to the south in the warmer scenario in comparison to the control scenario, approaching to the Canary Islands. This displacement could have increased the impacts over the archipelago. It is also worth noting the cyclone zonal acceleration in the middle of the simulated period, which happens earlier in +2SIM, as reflected in its velocity (Fig. S2a of the supplementary material).

The minimum SLP evolution (Fig. 2b) shows that HURDAT observations depict a notable drop followed by a steady increase until the final dissipation of the cyclone. CSIM shows a similar behaviour, although the minimum SLP drop is much less pronounced. However, HURDAT's observations (minimum SLP and maximum sustW10) may have uncertainties, since the resources employed by the NHC to collect the data from a Tropical Storm in the Northeastern Atlantic basin are fewer than for the tropical systems in the Western Atlantic (Beven, 2006; Knabb et al., 2023). Therefore, these deviations between the control simulation and observations could be not completely due to the numerical model. The minimum SLP in +2SIM (Fig. 2b) dropped notably in comparison to CSIM, depicting pressure values typical of hurricanes belonging to CAT. 2 (Simpson, 1974) from 27 November 03:00 UTC until 28 November 09:00 UTC. Once the ET starts, the minimum SLP weakens until it starts to dissipate before landfalling in Africa.

CSIM fits better with the maximum sustW10 observations from HURDAT, although it overestimates (underestimates) slightly before (after) the intensification on 27 November (Fig. 2c). +2SIM shows higher maximum sustW10 and lower minimum SLP which reflects a more intense cyclone. Specifically, Delta exhibits hurricane status maximum sustW10 values for two complete days from 27 November 04:00 UTC, peaking on 28 November 21:00 UTC with CAT. 3 wind speeds (183 km h^{-1}). The highest wind gust, 220 km h^{-1} (Fig. S2b of supplementary material), occurs when Delta is closest to the Canary Islands. This is relevant due to the increase in the socioeconomic impact in the islands in a future warmer scenario.

Delta's CPS reveals differences between the two scenarios during the initial days (Fig. 3). The symmetry parameter (B) shows slightly differences between the two simulations: the warmer Delta depicts slightly higher initial B values than the control Delta. In fact, in +2SIM, some isolated values exceed the threshold $B > 10$ m on 26 November (Fig. 3a), which would mark the start the ET (Hart, 2003). However, the following lower B values evidence that this was not indeed the start of the ET, as the $B = 10$ m threshold is an approximation and should not be taken so restrictively.

Regarding the thermal wind (V_T^U and V_T^L), CSIM exhibits a warm low-level core combined with a cold upper-level core (Fig. 3b), -i.e., a shallow warm core- a hybrid structure typical of subtropical cyclones (González-Alemán et al., 2015; Quitián-Hernández et al., 2021). In contrast, in +2SIM Delta develops a deep warm core, turning into a more tropical system. This is produced by the enhanced convection in the warmer scenario (see more in the Sect. 3.2.2), which promotes heating in higher levels in the troposphere, while the latent heat release in the control scenario is more reduced.

https://doi.org/10.5194/egusphere-2026-2701
Preprint. Discussion started: 22 May 2026

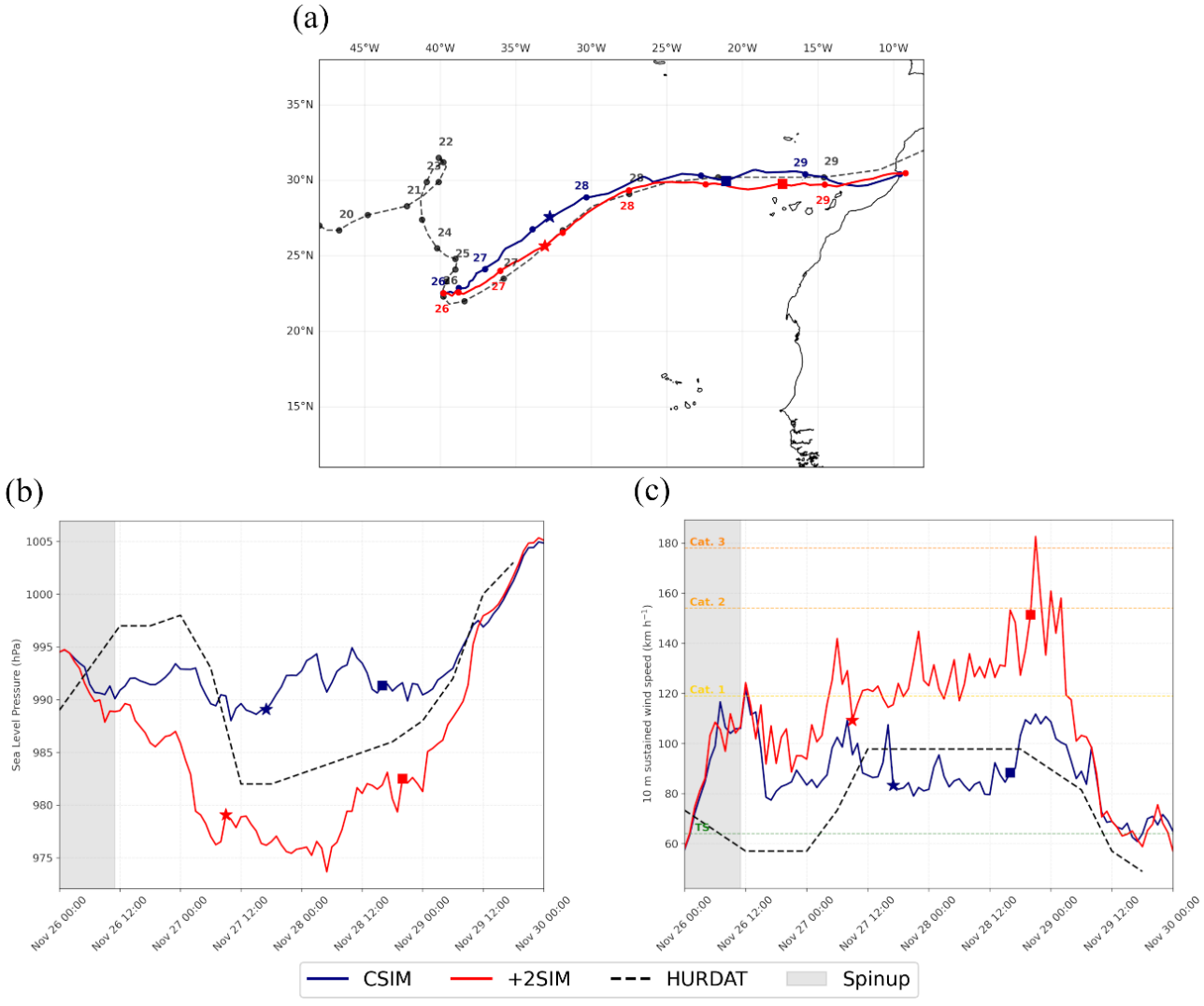

Figure 2: Comparison of different aspects of Delta in both simulations: (a) Trajectory, (b) minimum SLP, (c) maximum sustW10. In (a), dots indicate positions at 00:00 and 12:00 UTC, while day numbers are plotted at 00:00 UTC. Dotted black lines refer to the best track for Delta from HURDAT. The grey window indicates the first timesteps of the simulations, still influenced by the spinup. Horizontal dotted coloured lines in (c) indicate the thresholds for different TC categories in the Saffir-Simpson scale (The Saffir-Simpson Team et al., 2012). Stars and squares denote the beginning and the end of the ET, respectively, in both scenarios.

In +2SIM the cyclone starts to lose notably its horizontal symmetry on 27 November 09:00 UTC, while in CSIM Delta experiences this process about 8 h later. This highlights that the ET begins earlier in the warmer scenario. This is produced due to Delta being a more intense and vertically extended cyclone, which interacts earlier and more efficiently with the upper-level trough (Fig. S3 of supplementary material) and the vertical wind shear. However, this earlier start of the ET is not in line with what Ribberink et al. (2026) found when simulating Hurricane Ophelia (2017) with different perturbations in the atmospheric temperatures and the SSTs, where a larger warm-up resulted in a later ET beginning. The difference between results of Ribberink et al. (2026) and these may be in the asymmetric convective structure displayed by Delta (Fig.

https://doi.org/10.5194/egusphere-2026-2701
Preprint. Discussion started: 22 May 2026

3c) due to the dry intrusion produced by the MTD (explained in Sect. 3.1), while Ophelia kept an axisymmetric convection (Stewart, 2018).

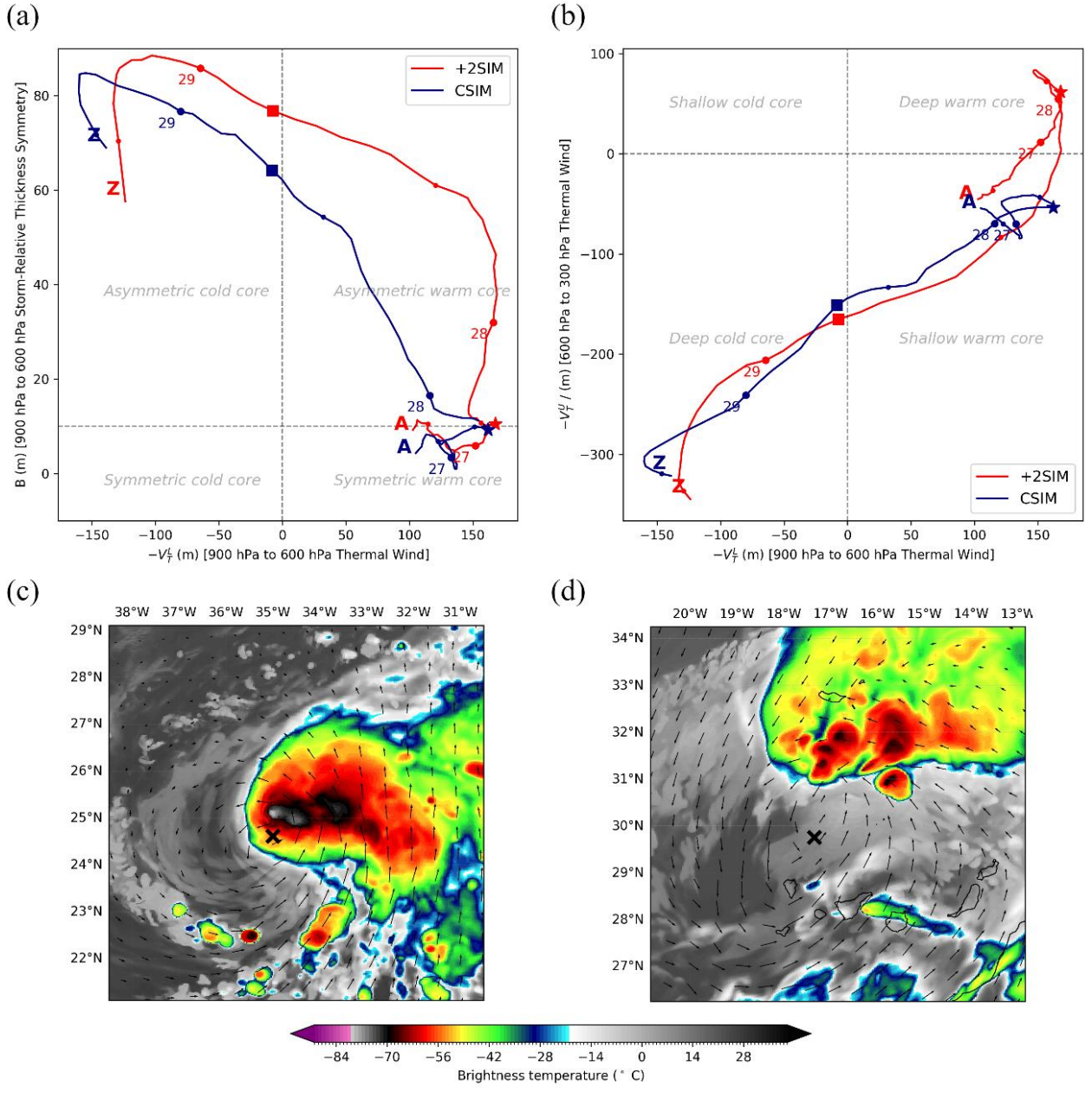

Figure 3: CPS diagrams for Delta in both simulations: (a) low-troposphere thermal wind vs thickness asymmetry, (b) low-troposphere thermal wind vs upper-troposphere thermal wind. Dots indicate positions in the CPS at 00:00 and 12:00 UTC, while day numbers are plotted at 00:00 UTC. A and Z mark initial and final positions, and stars and squares denote the beginning and the end of the ET, respectively. BT field at: (c) 04:00 UTC 27 November 2005, and (d) 20:00 UTC 28 November 2005, for +2SIM. Black arrows indicate 925 hPa wind vectors, and the black cross marks the cyclone's centre.

https://doi.org/10.5194/egusphere-2026-2701
Preprint. Discussion started: 22 May 2026

Asymmetric convection and diabatic heating generate asymmetric upward motions, that might modify the upper-level flows through asymmetric changes in potential vorticity associated with the diabatic heating (Davis et al., 2008; Riemer et al., 2010). These upper-level potential vorticity anomalies can increase the effective wind shear experienced by the cyclone (Grams & Archambault, 2016; Li et al., 2015), enhancing the loss of horizontal symmetry and favouring the development of a frontal structure. Delta's asymmetric convective structure (Fig. 3c), attained because of the dry intrusion, could amplify the initial thermal asymmetry in the CPS (Fig. 3a) through this mechanism. Meanwhile, in the case of Ophelia, although warmer SSTs would potentially intensify the cyclone and favour an earlier interaction with the upper-level trough and the wind shear, this mechanism may not be triggered due to its more axisymmetric structure and stronger vortex (Carr & Williams, 1989; Ribberink et al., 2026; Stewart, 2018). Therefore, the absence of a dry intrusion perturbing the convective structure might avoid the earlier start of the ET.

The period when Delta experiences the loss of thermal symmetry occurs when the zonal acceleration is produced in both scenarios (Fig. 2a, and Fig. S2a of supplementary material). This suggests that Delta's acceleration is caused by the beginning of the ET (Aiyyer & Wade, 2021; The COMET Program, 2009), after coupling with the upper-level trough (Fig. S3 in supplementary material).

Delta's transition to a thermally asymmetrical state occurs earlier in the warmer scenario, which means that the ET starts earlier. However, the transition to a cold core does not follow the same process. In CSIM, Delta experiences the transition from shallow warm core to deep cold core (from 00:00 UTC until 16:00 UTC 28 November) within a short time frame to the change from horizontally symmetrical to asymmetrical. These two processes seem to be less coupled in +2SIM, since the loss of symmetry happens earlier than in CSIM, and the complete cooling of the inner core occurs later. This process experienced by warmer Delta could be understood as a warm seclusion as it develops a frontal structure while retaining its deep warm tropical core. The traditional warm seclusion usually involves a pure extratropical cyclone whose warm front stretches backwards and the warm sector gets advected to the centre of the cyclone, developing a warm core (Shapiro & Keyser, 1990). The process in Delta would be a symmetric warm core developing a frontal structure. According to Sarro & Evans (2022), Delta would have suffered an instant warm seclusion. In +2SIM, Delta's upper core starts to cool on 28 November 00:00 UTC, followed by the low-level core around 10:00 UTC, while in CSIM the low-level core starts cooling at 00:00 UTC. The cooling in the lower levels is delayed for warmer Delta because the warm core has a larger vertical extension, and the upper levels are cooled first (top-down cooling). Therefore, the end of the ET (Fig. 3d) happens later, meaning that Delta remains with its tropical warm core longer. The ET duration is 23 h in CSIM (from 27 November 17:00 UTC to 28 November 16:00 UTC), increasing to 35 h in +2SIM (from 27 November 9:00 UTC to 28 November 20:00 UTC).

The beginning of the low-level cooling in the warmer climate coincides with the period during which the minimum SLP increased (Fig. 2b), while the maximum sustW10 are more intense (Fig. 2c). This maximum sustW10 experiences an increase of 66 km h^{-1} in 15 h since 28 November 06:00 UTC. These results show that the warmer SSTs do not make Delta a longer lasting system, since its central SLP weakens at the same time but creates a much more severe ET (Garin et al., 2025),

https://doi.org/10.5194/egusphere-2026-2701
Preprint. Discussion started: 22 May 2026

with rates of intensification in its wind speeds comparable to those of major hurricanes. These processes are extremely harmful to society and specially challenging to forecast with numerical weather prediction models (DeMaria et al., 2021). These results suggest that the increase in SSTs in the Northeastern Atlantic Ocean in future scenarios produced by ACC could cause ETs to be substantially more destructive (Garin et al., 2025). This is especially relevant since there are publications projecting an increase in the number of ETs produced in the North Atlantic in future scenarios (Baker et al., 2022; Michaelis & Lackmann, 2019).

3.2.2 Convective Activity

In this subsection the convection associated with Delta is studied, following the described methodology. As detailed previously, the main results correspond to the configuration of a 220 K external threshold and a 15 K step size (Fig. 4). The complete plots with the 16 combinations between external threshold and step are included in the supplementary material, although some of the results present in them will be referenced.

The time evolution of the number of convective cells is also studied, smoothed with running means in 5-hour windows. This is also a relevant metric to characterize convective activity itself in both scenarios. The number of convective cells in +2SIM, especially during the tropical phase, is larger than in CSIM (Fig. 4a). The evolution shows a decline in the number of cells as Delta turns extratropical. The number of cells grows as the external thresholds increase and the steps decrease (Fig. S4 of supplementary material), exhibiting a larger number of identified features under warmer conditions in all threshold-step combinations.

Figure 4a reflects an increase in the total and mean area of the convective cells in the +2SIM relative to CSIM. However, Fig. S4 of supplementary material indicates that the main behaviour is a reduction in the mean area of the convective cells, as shown by most of the threshold-step combinations. This reveals that the area exhibits high sensitivity to the thresholds utilized by Tobac to divide the convective cells. The lower mean area in the warmer scenario suggests greater fragmentation (Wasko et al., 2016), with more but smaller convective cells in the cyclone. Even so, nearly 69% of the step-threshold combinations (11 out of 16) show an increase in the total convective area in the warmer simulation, depicting a more organized convective structure with a larger horizontal extension, which is consistent with enhanced convective activity.

By increasing SSTs while leaving the atmospheric initial conditions unchanged, the surface fluxes get enhanced, warming and moistening the boundary layer. The associated rise in saturation specific humidity, consistent with Clausius-Clapeyron scaling (Fowler et al., 2021), implies higher specific humidity in the low levels. A significant increase in *WVFlux* ($\sqrt{u^2q^2 + v^2q^2}$; Guan & Waliser, 2015) is found within Delta's convective cells (Fig. 4b), showing a larger horizontal transport of moisture at lower levels (925 hPa) converging towards the centre of the cyclone (not shown). Herein, all the threshold-step combinations utilized to divide the cells show a shift in the distributions towards higher *WVFlux* values in +2SIM (Fig. S5 of supplementary material). This effect is particularly evident for the most restrictive external threshold (220 K), where the contribution from regions with negligible *WVFlux* is notably reduced.

https://doi.org/10.5194/egusphere-2026-2701
Preprint. Discussion started: 22 May 2026

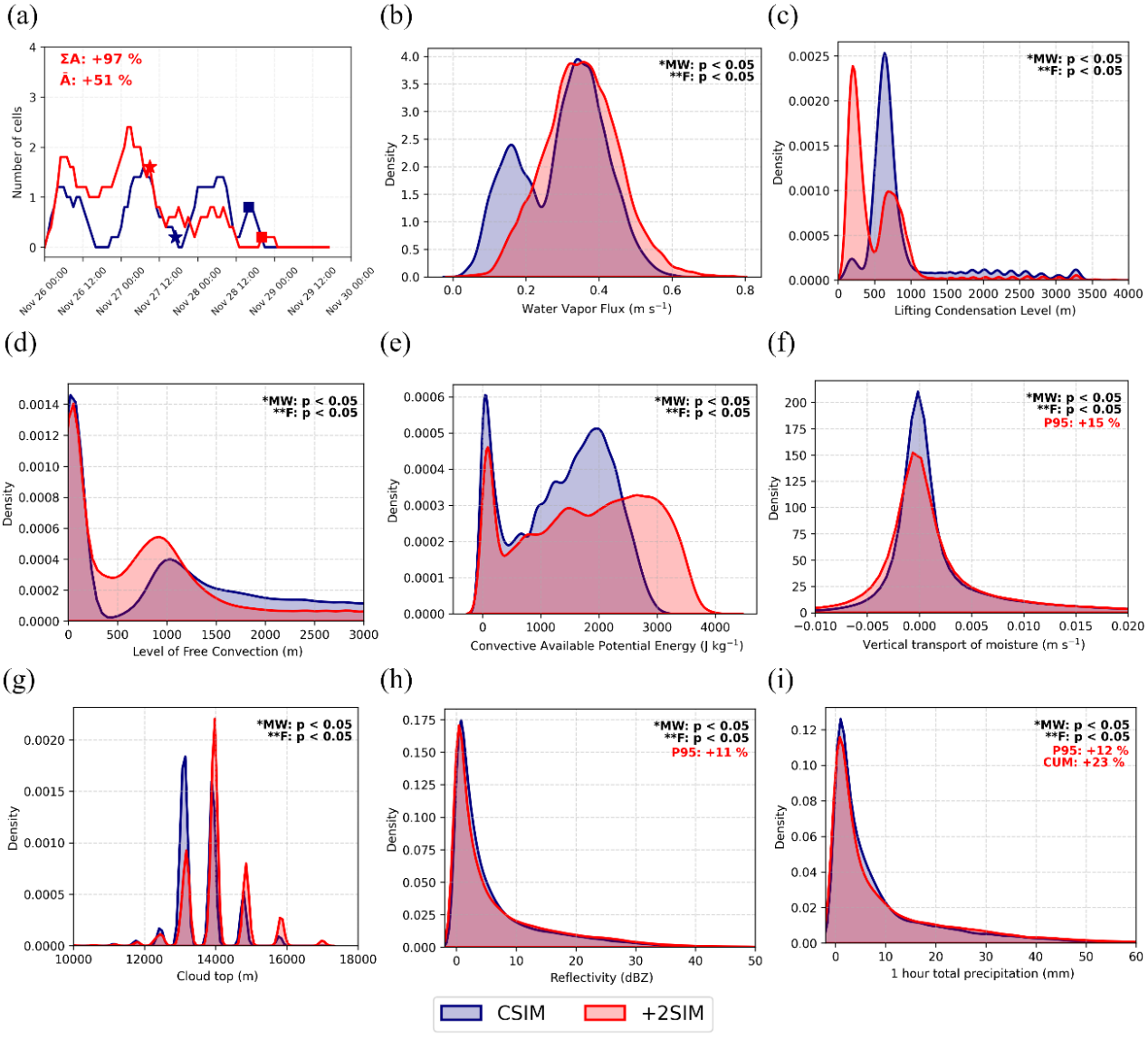

Figure 4: Comparison in both simulations of (a) Evolution of number of convective cells with CI identified in Delta, and PDFs for different variables within those convective cells: (b) *WVFlux* at 925 hPa (m s^{-1}), (c) LCL (m), (d) LFC (m), (e) CAPE (J kg^{-1}), (f) *wq* at 700 hPa (m s^{-1}), (g) CT (m), (h) Refl (dBZ), (i) TP (mm h^{-1}). Stars and squares in (a) denote the beginning and end of the ET, respectively, in both scenarios. In the top-right corner of the PDFs the symbol * denotes a significant difference in the distributions while two asterisks ** denote a significant difference in the variances, with p-values < 0.05 according to the Mann-Whitney and Fisher tests, respectively. In the top corners it is indicated the percentage of change in +2SIM relative to CSIM in: total and mean area of the convective cells in (a), 95th percentile of the distribution in (f), (h) and (i), and the total accumulated precipitation in the convective cells in (i); in red when it is an increase and blue when it is a decrease.

Thus, larger values of moisture are advected at low levels, providing more fuel for the convection. The increase in specific humidity leads to higher relative humidity, as the moisture increase outweighs the rise in saturation specific humidity associated with warmer air. Then, as parcels of warm air rise and approach saturation, the vertical distance travelled before

https://doi.org/10.5194/egusphere-2026-2701
Preprint. Discussion started: 22 May 2026

condensation begins is reduced. A significantly lower LCL is found in the warmer simulation (Fig. 4c and Fig. S6 of supplementary material), with the main peak decreasing from approximately 700 to 300 m. This increases the likelihood of air parcels rising adiabatically to reach their LCL without becoming colder than the surrounding environment. The larger the number of air parcels reaching the condensation increases the latent heat released, enhancing the convective updrafts (Markowski & Richardson, 2010).

Concerning the LFC, Fig. 4d displays LFC values in +2SIM significantly lower than in CSIM. The main change in the distributions is the emergence of LFC values around 500 m, at the expense of higher values above 1000 m, whose frequency gets reduced. Therefore, in +2SIM, a larger area exhibits a LFC located at relatively lower heights. Thus, in the warmer simulation more air parcels can reach their LFC during an updraft, allowing them to keep ascending due to their buoyancy until upper levels in the troposphere, which favours the development of deep moist convection. The frequency peaks at LFC values near 0 correspond to grid points without a defined LFC, associated with less convective regions within the clouds. Figure S7 of the supplementary material reflects a decrease in the relative contribution of these points to the overall distribution as the external BT threshold is reduced.

These changes in low-level water vapor, LCL and LFC are reflected in a significant increase in the CAPE in the convective cells over warmer SSTs (Fig. 4e), which is found statistically significant for all the BT thresholds and steps (Fig. S8 of supplementary material). The distribution of the CAPE in the convective cells increases substantially, with a large amount of grid points in the cells with values over 3000 J kg^{-1} in +2SIM, while this value is barely topped in CSIM. Thus, the increases in CAPE describe a thermodynamical environment in which deep moist convection is more likely to develop (Fischer & Knutti, 2015; Lepore et al., 2021; Markowski & Richardson, 2010).

This leads to several changes in the vertical transport of moisture within the convective cells (Fig. 4f) in the mid-troposphere (700 hPa). The distribution becomes significantly broader in +2SIM relative to CSIM, indicating a higher occurrence of the most extreme values of upward transport of moisture. A notable increase in the 95th percentile is found for almost all the threshold-step combinations (Fig. S9 of supplementary material). Accordingly, the highest *wq* values, corresponding to strong convective updrafts, appear more frequently over the warmer ocean. It is noteworthy that the highest negative values of the vertical transport of moisture also increase in this scenario, which could be associated to stronger downdrafts in the convective cells (Fig. 4f). This process may also play an important role in the development of convection, as enhanced downdrafts can promote the initiation of new convective cells through cold pool intensification (Marion & Trapp, 2019).

The enhanced convection in the surroundings of the cyclone's centre in the warmer scenario develops cumulonimbus clouds with a larger vertical extension (Fig. 4g). The main change in the distributions is the upward shift of a substantial fraction of points, from cloud top heights around 13000 m in CSIM to around 14000 m and higher in +2SIM, with the most extreme values reaching 17000 m. The discrete nature of these results arises from the vertical discretization in HARMONIE-AROME. This increase in cloud top is significant for all the thresholds and steps (Fig. S10 of supplementary material), meaning that even less convective regions are developing clouds until higher levels. This figure also supports the idea that 220 K is the best choice for the BT external threshold, since it erases almost all the contribution from clouds with tops under

https://doi.org/10.5194/egusphere-2026-2701
Preprint. Discussion started: 22 May 2026

12000 m. The increase in the vertical extension is also accompanied by an intensification in the highest reflectivity in the convective cells (Fig. 4h and Fig. S11 of supplementary material), as seen in the increase in the 95th percentile of the distribution in +2SIM.

These findings evidence that warmer SSTs provide more low-level moisture, fuelling convective activity within Tropical Storm Delta. Subsequently, this results in an increase in total precipitation in a 1 h period (Fig. 4i and Fig. S12 of supplementary material) in the convective cells from Fig. 4a, most of them living during Delta's tropical phase. The distributions display an increase in the appearance of the highest precipitation rates in +2SIM relative to CSIM for the majority of the thresholds and steps. In addition, considering the growth in the number of convective cells and their total area, the total accumulated precipitation under Delta's convective cells gets notably increased in +2SIM, rising a 67 % on average and with some threshold-step combinations even doubling the accumulated values from CSIM.

Moreover, Fig. 5 shows that the total accumulated precipitation caused by Delta during its whole lifecycle is greater in +2SIM than in CSIM, reaching higher values and displaying a larger affected area. In the warmer scenario, the total area accumulating over 50 mm of precipitation increases 50 %, and the area over 150 mm increases 118 %. Interestingly, the highest values of accumulated precipitation are produced in the second half of Delta's trajectory, once the ET is already started, especially north of the centre of the cyclone, where the convective structure was located (Fig. 3d). This result is particularly relevant in terms of the impacts associated with Delta, as its influence over the Canary Islands and Madeira occurred after it had fully transitioned into an extratropical baroclinic system.

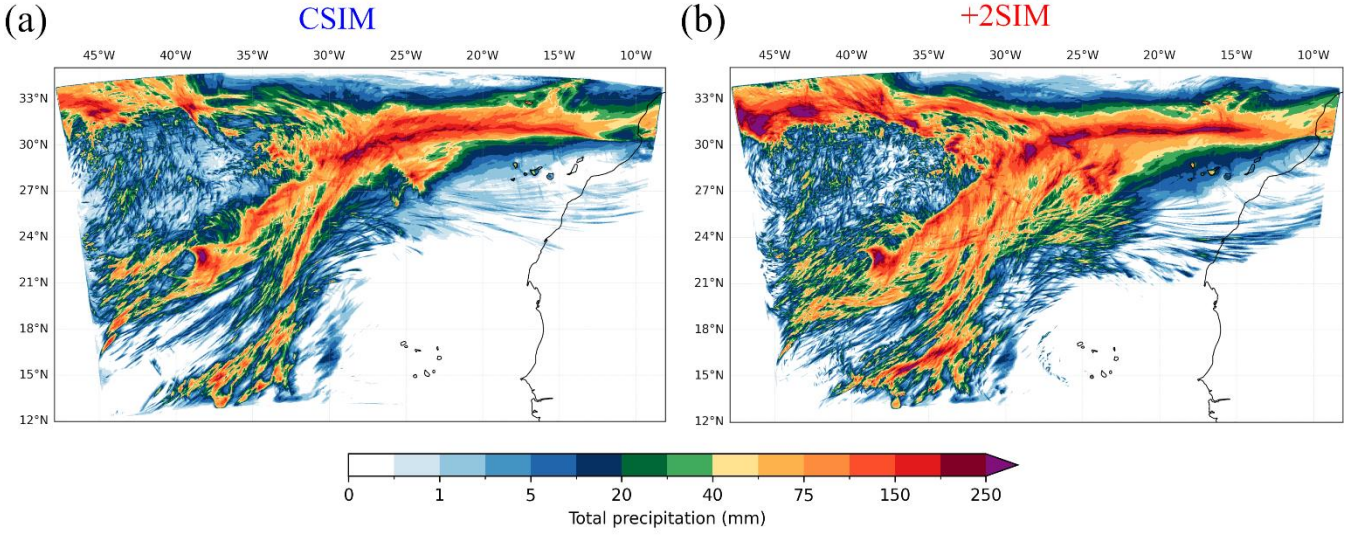

Figure 5: Total accumulated precipitation in the whole period for (a) CSIM, (b) +2SIM.

Finally, the minimum BT field (Fig. 6) displays the results previously explained for Fig. 4a and Fig. 4f, as the lowest BT values correspond to the convective cells analysed. The widespread greater convective activity over warmer SSTs is noticeable. During the tropical stage of the trajectory Delta exhibits a higher concentration of cells with colder tops below -

https://doi.org/10.5194/egusphere-2026-2701
Preprint. Discussion started: 22 May 2026

70 °C (~205 K) in +2SIM, showing the enhancement of convective updrafts. Once the ET begins, these cold cloud tops disappear, rendering the convection in Delta's dynamics irrelevant while the baroclinic contribution starts to become the main mechanism sustaining the cyclone. However, this does not happen in CSIM, where convective cells still reach cold tops during the ET. This means that diabatic processes due to convection remain relevant for a longer time in the control cyclone (Fig. 4a, and Fig. S4 of supplementary material). Thus, while the perturbed SSTs intensify convection during the tropical phase, they do not extend it over time. The TC strengthened by this convection turns into a more baroclinically-driven cyclone earlier due to the enhancement of its interaction with the jet stream.

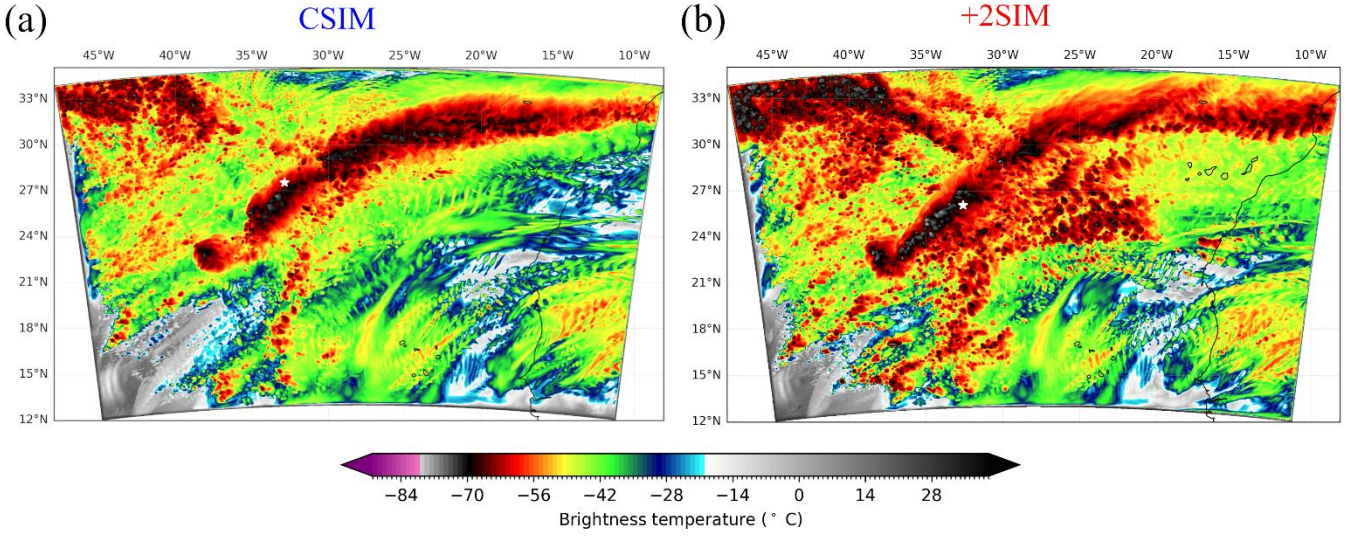

Figure 6: Minimum BT produced for (a) CSIM, (b) +2SIM. White stars denote the location of the beginning of the ET in each scenario.

Overall, the results shown here indicate a systematic intensification of convective activity under warmer ocean conditions, evidenced by the increased surface moisture fluxes, higher CAPE and enhanced updrafts within the convective cells associated with cyclone. These findings are consistent with previous studies suggesting enhanced convection and storm dynamics under future, warmer climates (e.g. Calvo-Sancho et al., 2026; Fowler et al., 2021; González-Alemán et al., 2023). This enhancement of convection in a warmer environment is strongly linked to the thermodynamic forcing provided by the ocean. Higher SSTs increase the saturation specific humidity at the surface following the Clausius-Clapeyron relationship (Fowler et al., 2021), which leads to an enhanced evaporation rate and air-sea latent heat fluxes. These processes promote an enhancement of low-level moisture (Fig. 4b), which plays a critical role in preconditioning the atmosphere for deep moist convection (Calvo-Sancho et al., 2026; Fowler et al., 2021; Markowski & Richardson, 2010). The increase in CAPE found in the simulations (Fig. 4e) most likely comes as a direct consequence of this enhanced low-level moistening. This is coherent with several studies finding important increases in CAPE in future, warmer climate scenarios (Fowler et al., 2021; Gensini et al., 2014; Lepore et al., 2021; Calvo-Sancho et al. 2026), describing environments more favourable for the development of deep moist convection.

https://doi.org/10.5194/egusphere-2026-2701
Preprint. Discussion started: 22 May 2026

Higher CAPE values are typically associated with stronger buoyancy, which supports more intense updrafts and enhances vertical mass transport within convective systems (Markowski & Richardson, 2010). These processes play a key role in the organization and maintenance of deep convection, particularly in highly organized systems such as mesoscale convective systems or TCs. In this context, Prein et al. (2021) reported an increase in upward moisture transport associated with stronger updrafts when simulating individual convective storms under future climate conditions. A similar behaviour is displayed in the simulations of Delta analysed in this study, where intense updrafts are more frequent, in accordance with an enhanced upward transport of moisture (Fig. 4f) and a more vigorous convective regime.

Consistent with the increased vertical moisture transport and stronger updrafts, a larger number of convective cells is found in the warmer scenario (Fig. 4a and Fig. 5), suggesting a larger atmospheric instability (González-Alemán et al., 2023; Martín et al., 2024). In addition, these individual cells are smaller in size, in agreement with Wasko et al. (2016), who reported reduced storm extents at higher temperatures, due to a redistribution of moisture towards the centres of the storms.

The intensification of convective activity and vertical moisture transport has direct implications for precipitation production. In this study, this is reflected in an intensification in hourly precipitation rates combined with a more widespread convection (Fig. 4i), which translates in a substantial increase in total accumulated precipitation under the system over warmer ocean conditions. Several previous studies project an increase in the rates of precipitation produced within mesoscale convective systems or cyclones in future climates (Ban et al., 2015; Fischer & Knutti, 2015; Fowler et al., 2021; Prein et al., 2017, 2021; Risser & Wehner, 2017; Wasko et al., 2016). A consistent response has been reported by Rios-Berrios et al. (2025), who found a substantial increase in daily precipitation in convection-permitting aquaplanet simulations when SSTs were increased, reinforcing the link between oceanic thermodynamic forcing and the overall enhancement of the hydrological response.

These results highlight that warmer ocean conditions enhance the thermodynamic environment for deep convection, specifically within a tropical cyclone. These findings contribute to a better understanding of how convective processes may respond to future warming across different convective systems, emphasizing that increases in accumulated precipitation and convective intensity are strongly linked to oceanic warming.

3 Summary and Conclusions

This study conducted a sensitivity analysis of the convective activity within Tropical Storm Delta, which affected the Canary Islands in November 2005. To this end, two simulations were performed using the HARMONIE-AROME mesoscale model: (i) a control simulation, with ERA5 initial and boundary conditions; and (ii) a perturbed simulation, in which a 2 ºC increase was added to the SSTs in the North Atlantic over which it developed, consistent with the observed SST trend in HadISST. The simulations are performed with the HARMONIE-AROME model, with a resolution that allows to resolve explicitly the deep convection in the cyclone. The analysis focuses on the convection in the convective cells within the inner region of the cyclone, which are objectively identified and tracked employing the Tobac package, based on some selected BT thresholds.

https://doi.org/10.5194/egusphere-2026-2701
Preprint. Discussion started: 22 May 2026

The results indicate that the warmer oceanic temperatures would create a warmer and more humid environment that would favour the buoyant ascents. The obtained results reflect lower LCL values that enhance latent heat release, as well as lower LFCs, promoting convective updrafts to upper levels, leading to an overall increase in CAPE and the potential for deep moist convection. Thus, the intensity, depth and extent of convective activity increase, as reflected by more frequent intense moist updrafts, higher cloud tops, larger precipitation rates, and a greater number and total area of convective cells associated to the cyclone. Some variables show sensitivity relative to the thresholds and steps used by Tobac to divide the individual convective cells, especially with those too large or loose that include non-convective regions, which should be had in consideration in future research employing a methodology to track convective cells including this package. Even so, the significant increase in the convection is found in the 16 combinations threshold-step utilized for the BT, corroborating the results in the main paper.

Therefore, the warmer SSTs induce an environment that enhances the convective activity in the surroundings of the cyclone's centre. This is coherent with previous works that project the midlatitudes to evolve towards thermodynamic conditions more susceptible to the development of deep moist convection (Fischer & Knutti, 2015; Lepore et al., 2021; Montoro-Mendoza et al., 2026).

The enhanced convection strengthens the cyclone through latent heat release and promotes its intensification during its tropical phase, which appears to favour an earlier and more efficient interaction with the upper-level trough and the vertical wind shear. Consequently, the cyclone loses its thermal symmetry earlier, favoured by its asymmetric convective structure due to a dry intrusion, and becomes baroclinically driven while maintaining a warm core for a longer time due to its larger vertical extension. This could be understood as an instant warm seclusion phase in its lifecycle.

Moreover, the intensification experienced by Delta due to a warmer SSTs produces a much more severe ET, with a larger precipitation area and especially stronger wind speeds, reaching hurricane values, and very harmful gusts over 200 km h^{-1}. This would be particularly impactful for the Canary Islands, as they were the main affected area by Delta's ET, although these findings are relevant for the whole Western Europe region, since a future TC approaching the area might not follow the same track and could make landfall in many different locations.

It is worth emphasizing that the warmer simulation analysed in this study is not dependent on a particular Shared Socioeconomic Pathway or on specific future emission trajectories. Instead, it explores a warming projected across a wide range of climate-change scenarios, grounded in the observed SST trend in the North Atlantic basin. Extrapolating this recent tendency suggests that a +2 ºC increase relative to November 2005 could be reached climatologically by the end of the century, and eventually earlier when considering internal variability. Therefore, the conditions examined here should be interpreted as a plausible continuation of recent observed changes rather than an extreme or unlikely future scenario.

Future research on this topic would include employing the Pseudo Global Warming Approach (Schär et al., 1996) to perturbate the atmospheric components too (temperatures, specific humidities, greenhouse gases and aerosol concentrations, …) besides the SSTs, according to CMIP6 climate projections. This could help to understand if the atmospheric contribution tends to increase even more the convection enhanced by the SSTs or if it is the opposite and the atmosphere tends to balance

https://doi.org/10.5194/egusphere-2026-2701
Preprint. Discussion started: 22 May 2026

back the increase caused by the ocean. In addition, performing an ensemble of simulations would allow to assess the uncertainties of the results and to further evaluate other aspects of the cyclone such as its dynamics and impacts.

To conclude, this work has shown that future climate scenarios with a warmer ocean would lead to an intensification of the convective activity and an enhancement of the diabatic processes within a TC, developing a much more severe system. Therefore, in future years a region like Western Europe could face the landfall of more violent and impactful cyclones, evidencing the urgent need for stronger political action to reduce and mitigate ACC, as such events would likely lead to major human losses and socioeconomic damage.

Code and data availability

Data from the ERA5 reanalysis are publicly available through the Copernicus Climate Data Store: https://cds.climate.copernicus.eu/datasets. The HURDAT2 database provided by the NHC is available online at: https://www.aoml.noaa.gov/hrd/hurdat/hurdat2.html. The HadISST dataset from the Met Office is also available online at: https://www.metoffice.gov.uk/hadobs/hadisst/data/download.html. The Tobac package used in this study is openly available on GitHub: https://github.com/tobac-project/tobac. HARMONIE-AROME model outputs, together with the analysis and visualization scripts developed for this work, are available from the corresponding author upon reasonable request.

Author contributions

Conceptualization: JJGA, MLM, PGP. Supervision: MLM, CCS, JJGA. Data curation: PGP, JJGA, EJRA, JDF. Formal analysis: PGP, EJRA, AMM. Software: PGP, CCS, JJGA; Project administration: MLM, IG. Validation: MLM, PB, JJGA, CCS, IG. Writing original draft: PGP. Writing review and edits: MLM, JDF, CCS, IG, JJGA.

Competing interests

The contact author has declared that none of the authors has any competing interests.

Disclaimer

Copernicus Publications remains neutral with regard to jurisdictional claims made in the text, published maps, institutional affiliations, or any other geographical representation in this paper. While Copernicus Publications makes every effort to

https://doi.org/10.5194/egusphere-2026-2701
Preprint. Discussion started: 22 May 2026

include appropriate place names, the final responsibility lies with the authors. Views expressed in the text are those of the authors and do not necessarily reflect the views of the publisher.

Acknowledgements

This research received support from the CONSCIENCE project (PID2023-146344OB-I00), funded by the Spanish Ministry of Science, Innovation and Universities (MICIU/AEI/10.13039/501100011033) and by FEDER-EU and by EU and the ECMWF Special Projects SPESMART, SPESVALE and SPESSANC. P. Gómez Plasencia acknowledges funding from the CONSCIENCE project (PID2023-146344OB-I00) and associated research contract CP25/138. E. J. Rodríguez-Acosta acknowledges the grant awarded by the Spanish Ministry of Science and Innovation - FPI program (PREP2023-001177). C. Calvo-Sancho acknowledges support from the GVA. PROMETEO Grant CIPROM/2023/38; and CSIC-LINCGLOBAL Ref. LINCG24042. J.J. González-Alemán thanks support from the Spanish State Meteorological Agency.

Financial support

This research has been supported by the Ministerio de Ciencia e Innovación (grant nos. PID2023-146344OBI00) and the European Centre for Medium Range Weather Forecasts (grant nos. SPESMART, SPESVALE and SPESSANC).

References

Aiyyer, A., & Wade, T. (2021). Acceleration of tropical cyclones as a proxy for extratropical interactions: synoptic-scale patterns and long-term trends. Weather and Climate Dynamics, 2(4), 1051–1072. https://doi.org/10.5194/wcd-2-1051-2021

Allan, D. B., Caswell, T., Keim, N. C., van der Wel, C. M., & Verweij, R. W. (2021). soft-matter/trackpy: Trackpy v0.5.0 (v0.5.0). Zenodo. https://doi.org/10.5281/zenodo.4682814

Baatsen, M., Haarsma, R. J., Van Delden, A. J., & de Vries, H. (2015). Severe Autumn storms in future Western Europe with a warmer Atlantic Ocean. Climate Dynamics, 45(3–4), 949–964. https://doi.org/10.1007/s00382-014-2329-8

Baker, A. J., Roberts, M. J., Vidale, P. L., Hodges, K. I., Seddon, J., Vannière, B., Haarsma, R. J., Schiemann, R., Kapetanakis, D., Tourigny, E., Lohmann, K., Roberts, C. D., & Terray, L. (2022). Extratropical Transition of Tropical Cyclones in a Multiresolution Ensemble of Atmosphere-Only and Fully Coupled Global Climate Models. Journal of Climate, 35(16), 5283–5306. https://doi.org/10.1175/JCLI-D-21-0801.1

Ban, N., Schmidli, J., & Schär, C. (2015). Heavy precipitation in a changing climate: Does short-term summer precipitation increase faster? Geophysical Research Letters, 42(4), 1165–1172. https://doi.org/10.1002/2014GL062588

https://doi.org/10.5194/egusphere-2026-2701
Preprint. Discussion started: 22 May 2026

Bengtsson, L., Andrae, U., Aspelien, T., Batrak, Y., Calvo, J., Rooy, W. de, Gleeson, E., Hansen-Sass, B., Homleid, M., Hortal, M., Ivarsson, K. I., Lenderink, G., Niemelä, S., Nielsen, K. P., Onvlee, J., Rontu, L., Samuelsson, P., Muñoz, D. S., Subias, A., … Køltzow, M. Ø. (2017). The HARMONIE-AROME model configuration in the ALADIN-HIRLAM NWP system. Monthly Weather Review, 145(5), 1919–1935. https://doi.org/10.1175/MWR-D-16-0417.1

Beven, J. (2006). Tropical Cyclone Report: Tropical Storm Delta, 22 - 28 November 2005. https://www.nhc.noaa.gov/data/tcr/AL292005_Delta.pdf

Bisgaard, S., & Vardeman, S. B. (1995). Statistics for Engineering Problem Solving. In The American Statistician (Number 3). https://doi.org/10.2307/2684208

Browning, K. A., Thorpe, A. J., Montani, A., Parsons, D., Griffiths, M., Panagi, P., & Dicks, E. M. (2000). Interactions of Tropopause Depressions with an Ex–Tropical Cyclone and Sensitivity of Forecasts to Analysis Errors. Monthly Weather Review, 128(8), 2734–2755. https://doi.org/10.1175/1520-0493(2000)128<2734:IOTDWA>2.0.CO;2

Calvo-Sancho, C., Díaz-Fernández, J., González-Alemán, J. J., Halifa-Marín, A., Miglietta, M. M., Azorin-Molina, C., Prein, A. F., Montoro-Mendoza, A., Bolgiani, P., Morata, A., & Martín, M. L. (2026). Human-induced climate change amplification on storm dynamics in Valencia's 2024 catastrophic flash flood. Nature Communications, 17(1), 1492. https://doi.org/10.1038/s41467-026-68929-9

Calvo-Sancho, C., Quitián-Hernández, L., González-Alemán, J. J., Bolgiani, P., Santos-Muñoz, D., & Martín, M. L. (2023). Assessing the performance of the HARMONIE-AROME and WRF-ARW numerical models in North Atlantic Tropical Transitions. Atmospheric Research, 291. https://doi.org/10.1016/j.atmosres.2023.106801

Camargo, S. J., Murakami, H., Bloemendaal, N., Chand, S. S., Deshpande, M. S., Dominguez-Sarmiento, C., González-Alemán, J. J., Knutson, T. R., Lin, I. I., Moon, I. J., Patricola, C. M., Reed, K. A., Roberts, M. J., Scoccimarro, E., Tam, C. Y. (Francis), Wallace, E. J., Wu, L., Yamada, Y., Zhang, W., & Zhao, H. (2023). An update on the influence of natural climate variability and anthropogenic climate change on tropical cyclones. Tropical Cyclone Research and Review, 12(3), 216–239. https://doi.org/10.1016/j.tcrr.2023.10.001

Carr, L. E., & Williams, R. T. (1989). Barotropic Vortex Stability to Perturbations from Axisymmetry. Journal of the Atmospheric Sciences, 46(20), 3177–3191. https://doi.org/10.1175/1520-0469(1989)046<3177:BVSTPF>2.0.CO;2

Collins, M., Knutti, R., Arblaster, J., Dufresne, J.-L., Fichefet, T., Friedlingstein, P., Gao, X., Gutowski, W., Johns, T., Krinner, G., Shongwe, M., Tebaldi, C., Weaver, A., & Wehner, M. (2013). Long-term Climate Change: Projections, Commitments and Irreversibility. In: Climate Change 2013: The Physical Science Basis. Contribution of Working Group I to the Fifth Assessment Report of the Intergovernmental Panel on Climate Change [Stocker, T.F., D. Qin, G.-K. Plattner, M. Tignor, S.K. Allen, J. Boschung, A. Nauels, Y. Xia, V. Bex and P.M. Midgley (eds.)]. Cambridge University Press, Cambridge, United Kingdom and New York, NY, USA. https://www.ipcc.ch/site/assets/uploads/2018/02/WG1AR5_Chapter12_FINAL.pdf

https://doi.org/10.5194/egusphere-2026-2701
Preprint. Discussion started: 22 May 2026

Da Costa Têso, J. M. (2006). CONSIDERAÇÕES SOBRE A TEMPESTADE TROPICAL DELTA E INFLUÊNCIA NA REGIÃO AUTÓNOMA DA MADEIRA. https://www.ipma.pt/export/sites/ipma/bin/docs/relatorios/meteorologia/rm.int_tempestade.tropical.delta.pdf

Dare, R. A., & McBride, J. L. (2011). The Threshold Sea Surface Temperature Condition for Tropical Cyclogenesis. Journal of Climate, 24(17), 4570–4576. https://doi.org/10.1175/JCLI-D-10-05006.1

Davis, C. A., & Bosart, L. F. (2004). Baroclinically Induced Tropical Cyclogenesis. Monthly Weather Review, 131(11). https://doi.org/https://doi.org/10.1175/1520-0493(2003)131<2730:BITC>2.0.CO;2

Davis, C. A., Jones, S. C., & Riemer, M. (2008). Hurricane Vortex Dynamics during Atlantic Extratropical Transition. Journal of the Atmospheric Sciences, 65(3), 714–736. https://doi.org/10.1175/2007JAS2488.1

Dekker, M. M., Haarsma, R. J., Vries, H. de, Baatsen, M., & Delden, A. J. van. (2018). Characteristics and development of European cyclones with tropical origin in reanalysis data. Climate Dynamics, 50(1–2), 445–455. https://doi.org/10.1007/s00382-017-3619-8

DeMaria, M., Franklin, J. L., Onderlinde, M. J., & Kaplan, J. (2021). Operational Forecasting of Tropical Cyclone Rapid Intensification at the National Hurricane Center. Atmosphere, 12(6), 683. https://doi.org/10.3390/atmos12060683

Díaz-Fernández, J., Bolgiani, P., Santos-Muñoz, D., Quitián-Hernández, L., Sastre, M., Valero, F., Farrán, J. I., González-Alemán, J. J., & Martín, M. L. (2022). Comparison of the WRF and HARMONIE models ability for mountain wave warnings. Atmospheric Research, 265. https://doi.org/10.1016/j.atmosres.2021.105890

Dirksen, M., Wijnant, I., Siebesma, A. P., Baas, P., & Theeuwes, N. E. (2022). Validation of wind farm parameterisation in Weather Forecast Model HARMONIE-AROME: Analysis of 2019. https://www.wins50.nl/publications/

Emanuel, K. (2021). Atlantic tropical cyclones downscaled from climate reanalyses show increasing activity over past 150 years. Nature Communications, 12(1). https://doi.org/10.1038/s41467-021-27364-8

Evans, C., Wood, K. M., Aberson, S. D., Archambault, H. M., Milrad, S. M., Bosart, L. F., Corbosiero, K. L., Davis, C. A., Pinto, J. R. D., Doyle, J., Fogarty, C., Galarneau, T. J., Grams, C. M., Griffin, K. S., Gyakum, J., Hart, R. E., Kitabatake, N., Lentink, H. S., Mctaggart-Cowan, R., … Zhang, F. (2017). The extratropical transition of tropical cyclones. Part I: Cyclone evolution and direct impacts. In Monthly Weather Review (Vol. 145, Number 11, pp. 4317–4344). American Meteorological Society. https://doi.org/10.1175/mwr-d-17-0027.1

Eyring, V., Bony, S., Meehl, G. A., Senior, C. A., Stevens, B., Stouffer, R. J., & Taylor, K. E. (2016). Overview of the Coupled Model Intercomparison Project Phase 6 (CMIP6) experimental design and organization. Geoscientific Model Development, 9(5), 1937–1958. https://doi.org/10.5194/gmd-9-1937-2016

Fischer, E. M., & Knutti, R. (2015). Anthropogenic contribution to global occurrence of heavy-precipitation and high-temperature extremes. Nature Climate Change, 5(6), 560–564. https://doi.org/10.1038/nclimate2617

Fowler, H. J., Lenderink, G., Prein, A. F., Westra, S., Allan, R. P., Ban, N., Barbero, R., Berg, P., Blenkinsop, S., Do, H. X., Guerreiro, S., Haerter, J. O., Kendon, E. J., Lewis, E., Schaer, C., Sharma, A., Villarini, G., Wasko, C., & Zhang, X. (2021).

https://doi.org/10.5194/egusphere-2026-2701
Preprint. Discussion started: 22 May 2026

Anthropogenic intensification of short-duration rainfall extremes. Nature Reviews Earth & Environment, 2(2), 107–122. https://doi.org/10.1038/s43017-020-00128-6

Garin, A., Pausata, F. S. R., Boudreault, M., & Ingrosso, R. (2025). The impacts of climate change on tropical-to-extratropical transitions in the North Atlantic Basin. Weather and Climate Dynamics, 6(4), 1379–1397. https://doi.org/10.5194/wcd-6-1379-2025

Gensini, V. A., Ramseyer, C., & Mote, T. L. (2014). Future convective environments using NARCCAP. International Journal of Climatology, 34(5), 1699–1705. https://doi.org/10.1002/joc.3769

González-Alemán, J. J., Insua-Costa, D., Bazile, E., González-Herrero, S., Miglietta, M. M., Groenemeijer, P., & Donat, M. G. (2023). Anthropogenic Warming Had a Crucial Role in Triggering the Historic and Destructive Mediterranean Derecho in Summer 2022. Bulletin of the American Meteorological Society, 104(8), E1526–E1532. https://doi.org/10.1175/BAMS-D-23-0119.1

González-Alemán, J. J., Valero, F., Martín-León, F., & Evans, J. L. (2015). Classification and Synoptic Analysis of Subtropical Cyclones within the Northeastern Atlantic Ocean*. Journal of Climate, 28(8), 3331–3352. https://doi.org/10.1175/JCLI-D-14-00276.1

Grams, C. M., & Archambault, H. M. (2016). The Key Role of Diabatic Outflow in Amplifying the Midlatitude Flow: A Representative Case Study of Weather Systems Surrounding Western North Pacific Extratropical Transition. Monthly Weather Review, 144(10), 3847–3869. https://doi.org/10.1175/MWR-D-15-0419.1

Guan, B., & Waliser, D. E. (2015). Detection of atmospheric rivers: Evaluation and application of an algorithm for global studies. Journal of Geophysical Research: Atmospheres, 120(24), 12514–12535. https://doi.org/10.1002/2015JD024257

Haarsma, R. J., Hazeleger, W., Severijns, C., De Vries, H., Sterl, A., Bintanja, R., Van Oldenborgh, G. J., & Van Den Brink, H. W. (2013). More hurricanes to hit western Europe due to global warming. Geophysical Research Letters, 40(9), 1783–1788. https://doi.org/10.1002/grl.50360

Hart, R. E. (2003). A Cyclone Phase Space Derived from Thermal Wind and Thermal Asymmetry. Monthly Weather Review, 131(4). https://doi.org/10.1175/1520-0493(2003)131<0585:ACPSDF>2.0.CO;2

Heikenfeld, M., Marinescu, P. J., Christensen, M., Watson-Parris, D., Senf, F., Van Den Heever, S. C., & Stier, P. (2019). Tobac 1.2: Towards a flexible framework for tracking and analysis of clouds in diverse datasets. Geoscientific Model Development, 12(11), 4551–4570. https://doi.org/10.5194/gmd-12-4551-2019

Henderson, D. S., Otkin, J. A., & Mecikalski, J. R. (2021). Evaluating convective initiation in high-resolution numerical weather prediction models using GOES-16 infrared brightness temperatures. Monthly Weather Review, 149(4), 1153–1172. https://doi.org/10.1175/MWR-D-20-0272.1

Hersbach, H., Bell, B., Berrisford, P., & et al. (2023). ERA5 hourly data on single levels from 1940 to present. https://doi.org/10.24381/cds.adbb2d47

Holland, G., & Bruyère, C. L. (2014). Recent intense hurricane response to global climate change. Climate Dynamics, 42(3–4), 617–627. https://doi.org/10.1007/s00382-013-1713-0

https://doi.org/10.5194/egusphere-2026-2701
Preprint. Discussion started: 22 May 2026

IPCC. (2023). Climate Change 2023: Synthesis Report. Contribution of Working Groups I, II and III to the Sixth Assessment Report of the Intergovernmental Panel on Climate Change [Core Writing Team, H. Lee and J. Romero (eds.)]. IPCC, Geneva, Switzerland (P. Arias, M. Bustamante, I. Elgizouli, G. Flato, M. Howden, C. Méndez-Vallejo, J. J. Pereira, R. Pichs-Madruga, S. K. Rose, Y. Saheb, R. Sánchez Rodríguez, D. Ürge-Vorsatz, C. Xiao, N. Yassaa, J. Romero, J. Kim, E. F. Haites, Y. Jung, R. Stavins, … C. Péan, Eds.). https://doi.org/10.59327/IPCC/AR6-9789291691647

Knabb, R. D., Rhome, J. R., & Browm, D. P. (2023). Tropical Cyclone Report: Hurricane Katrina, 23 - 30 August 2005. https://www.nhc.noaa.gov/data/tcr/AL122005_Katrina.pdf

Landsea, C. W., & Franklin, J. L. (2013). Atlantic Hurricane Database Uncertainty and Presentation of a New Database Format. Monthly Weather Review, 141(10), 3576–3592. https://doi.org/10.1175/MWR-D-12-00254.1

Lepore, C., Abernathey, R., Henderson, N., Allen, J. T., & Tippett, M. K. (2021). Future Global Convective Environments in CMIP6 Models. Earth's Future, 9(12). https://doi.org/10.1029/2021EF002277

Leung, G. R., Saleeby, S. M., Sokolowsky, G. A., Freeman, S. W., & van den Heever, S. C. (2023). Aerosol–cloud impacts on aerosol detrainment and rainout in shallow maritime tropical clouds. Atmospheric Chemistry and Physics, 23(9), 5263–5278. https://doi.org/10.5194/acp-23-5263-2023

Li, Y., Cheung, K. K. W., & Chan, J. C. L. (2015). Modelling the effects of land–sea contrast on tropical cyclone precipitation under environmental vertical wind shear. Quarterly Journal of the Royal Meteorological Society, 141(687), 396–412. https://doi.org/10.1002/qj.2359

Lima, M. M., Hurduc, A., Ramos, A. M., & Trigo, R. M. (2021). The Increasing Frequency of Tropical Cyclones in the Northeastern Atlantic Sector. Frontiers in Earth Science, 9. https://doi.org/10.3389/feart.2021.745115

Mann, H. B., & Whitney, D. R. (1947). On a Test of Whether one of Two Random Variables is Stochastically Larger than the Other. The Annals of Mathematical Statistics, 18(1), 50–60. https://doi.org/10.1214/aoms/1177730491

Marion, G. R., & Trapp, R. J. (2019). The Dynamical Coupling of Convective Updrafts, Downdrafts, and Cold Pools in Simulated Supercell Thunderstorms. Journal of Geophysical Research: Atmospheres, 124(2), 664–683. https://doi.org/10.1029/2018JD029055

Markowski, Paul., & Richardson, Yvette. (2010). Mesoscale meteorology in midlatitudes. Wiley-Blackwell.

Martín León, F., Alejo Herrera, C. J., Bustos Seguela, J. J. de, Calvo Sánchez, F. J., San Ambrosio Beirán, J. I., Sánchez-Laulhé, J. M., & Santos Muñoz, D. (2005). Arcimis: Estudio de la tormenta tropical "Delta" y su transición extratropical: efectos meteorológicos en Canarias. Agencia Estatal de Meteorología. http://hdl.handle.net/20.500.11765/1341

Martín, M. L., Calvo-Sancho, C., Taszarek, M., González-Alemán, J. J., Montoro-Mendoza, A., Díaz-Fernández, J., Bolgiani, P., Sastre, M., & Martín, Y. (2024). Major Role of Marine Heatwave and Anthropogenic Climate Change on a Giant Hail Event in Spain. Geophysical Research Letters, 51(6). https://doi.org/10.1029/2023GL107632

Michaelis, A. C., & Lackmann, G. M. (2019). Climatological Changes in the Extratropical Transition of Tropical Cyclones in High-Resolution Global Simulations. Journal of Climate, 32(24), 8733–8753. https://doi.org/10.1175/JCLI-D-19-0259.1

https://doi.org/10.5194/egusphere-2026-2701
Preprint. Discussion started: 22 May 2026

Montoro-Mendoza, A., Calvo-Sancho, C., González-Alemán, J. J., Díaz-Fernández, J., Bolgiani, P., & Martín, M. L. (2026). Strengthening of favorable environments for North Atlantic tropical cyclogenesis in midlatitudes in a warmer climate. Npj Climate and Atmospheric Science. https://doi.org/10.1038/s41612-025-01317-0

Murakami, H., & Wang, B. (2010). Future change of North Atlantic tropical cyclone tracks: Projection by a 20-km-mesh global atmospheric model. Journal of Climate, 23(10), 2699–2721. https://doi.org/10.1175/2010JCLI3338.1

Oouchi, K., Yoshimura, J., Yoshimura, H., Kusunoki, S., & Noda, A. (2006). Tropical Cyclone Climatology in a Global-Warming Climate as Simulated in a 20 km-Mesh Global Atmospheric Model: Frequency and Wind Intensity Analyses. Journal of the Meteorological Society of Japan, 84(2), 259–276. https://doi.org/https://doi.org/10.2151/jmsj.84.259

Parlamento de Canarias. (2006). Resolución de la Comisión de Investigación del Parlamento de Canarias de la Tormenta Tropical Delta. Boletín Oficial del Parlamento de Canarias. https://www.parcan.es//pub/bop/6l/2006/371/bo371.pdf

Pasch, R. J., & Roberts, D. P. (2018). Tropical Cyclone Report: Hurricane Leslie, 23 September - 13 October 2018. https://www.nhc.noaa.gov/data/tcr/AL132018_Leslie.pdf

Prein, A. F., Liu, C., Ikeda, K., Trier, S. B., Rasmussen, R. M., Holland, G. J., & Clark, M. P. (2017). Increased rainfall volume from future convective storms in the US. Nature Climate Change, 7(12), 880–884. https://doi.org/10.1038/s41558-017-0007-7

Prein, A. F., Rasmussen, R. M., Wang, D., & Giangrande, S. E. (2021). Sensitivity of organized convective storms to model grid spacing in current and future climates. Philosophical Transactions of the Royal Society A: Mathematical, Physical and Engineering Sciences, 379(2195), 20190546. https://doi.org/10.1098/rsta.2019.0546

Quitián-Hernández, L., Bolgiani, P., Santos-Muñoz, D., Sastre, M., Díaz-Fernández, J., González-Alemán, J. J., Farrán, J. I., Lopez, L., Valero, F., & Martín, M. L. (2021). Analysis of the October 2014 subtropical cyclone using the WRF and the HARMONIE-AROME numerical models: Assessment against observations. Atmospheric Research, 260, 105697. https://doi.org/10.1016/j.atmosres.2021.105697

Rayner, N. A., Parker, D. E., Horton, E. B., Folland, C. K., Alexander, L. V., Rowell, D. P., Kent, E. C., & Kaplan, A. (2003). Global analyses of sea surface temperature, sea ice, and night marine air temperature since the late nineteenth century. Journal of Geophysical Research: Atmospheres, 108(D14). https://doi.org/10.1029/2002JD002670

Reinhart, B. J. (2023). Tropical Cyclone Report: Tropical Storm Hermine, 23 - 24 September 2022. https://www.nhc.noaa.gov/data/tcr/AL102022_Hermine.pdf

Ribberink, M., de Vries, H., Bloemendaal, N., Baatsen, M., & van Meijgaard, E. (2026). Tropical cyclone intensification and extratropical transition under alternate climate conditions: a case study of Hurricane Ophelia (2017). Weather and Climate Dynamics, 7(1), 37–64. https://doi.org/10.5194/wcd-7-37-2026

Riehl, H. (1954). Tropical Meteorology. McGraw-Hill.

Riemer, M., Montgomery, M. T., & Nicholls, M. E. (2010). A new paradigm for intensity modification of tropical cyclones: thermodynamic impact of vertical wind shear on the inflow layer. Atmospheric Chemistry and Physics, 10(7), 3163–3188. https://doi.org/10.5194/acp-10-3163-2010

https://doi.org/10.5194/egusphere-2026-2701
Preprint. Discussion started: 22 May 2026

Rios-Berrios, R., Emanuel, K., Bryan, G. H., Medeiros, B., & Done, J. (2025). Response of Tropical Climate and Extreme Precipitation to Ocean Temperature in Convection-Permitting Aquaplanet Simulations. Journal of Advances in Modeling Earth Systems, 17(10). https://doi.org/10.1029/2025MS005119

Rios-Berrios, R., Finocchio, P. M., Alland, J. J., Chen, X., Fischer, M. S., Stevenson, S. N., & Tao, D. (2024). A Review of the Interactions between Tropical Cyclones and Environmental Vertical Wind Shear. Journal of the Atmospheric Sciences, 81(4), 713–741. https://doi.org/10.1175/JAS-D-23-0022.1

Risser, M. D., & Wehner, M. F. (2017). Attributable Human-Induced Changes in the Likelihood and Magnitude of the Observed Extreme Precipitation during Hurricane Harvey. Geophysical Research Letters, 44(24). https://doi.org/10.1002/2017GL075888

Roberts, M. J., Camp, J., Seddon, J., Vidale, P. L., Hodges, K., Vannière, B., Mecking, J., Haarsma, R., Bellucci, A., Scoccimarro, E., Caron, L., Chauvin, F., Terray, L., Valcke, S., Moine, M., Putrasahan, D., Roberts, C. D., Senan, R., Zarzycki, C., … Wu, L. (2020). Projected Future Changes in Tropical Cyclones Using the CMIP6 HighResMIP Multimodel Ensemble. Geophysical Research Letters, 47(14). https://doi.org/10.1029/2020GL088662

Sampson, C. R., Jeffries, R. A., Neumann, C. J., & Chu, J.-H. (1995). Chapter 6. Tropical Cyclone Intensity. Section 2.2. Wind Speed Averaging Times. In Tropical Cyclone Forecasters Reference Guide. Naval Research Laboratory. https://web.archive.org/web/20070916205204/http:/www.nrlmry.navy.mil/~chu/chap6/se200.htm

Sarro, G., & Evans, C. (2022). An Updated Investigation of Post-Transformation Intensity, Structural, and Duration Extremes for Extratropically Transitioning North Atlantic Tropical Cyclones. Monthly Weather Review, 150(11), 2911–2933. https://doi.org/10.1175/MWR-D-22-0088.1

Schär, C., Frei, C., Lüthi, D., & Davies, H. C. (1996). Surrogate climate-change scenarios for regional climate models. Geophysical Research Letters, 23(6), 669–672. https://doi.org/10.1029/96GL00265

Shapiro, M. A., & Keyser, D. (1990). Fronts, jet streams, and the tropopause. In C. W. Newton & E. O. Holopainen (Eds.), Extratropical Cyclones: The Erik Palmén Memorial Volume (pp. 167–191). American Meteorological Society.

Simpson, R. H. (1974). The Hurricane Disaster—Potential Scale. Weatherwise, 27(4), 169–186. https://doi.org/10.1080/00431672.1974.9931702

Sokolowsky, G. A., Freeman, S. W., Jones, W. K., Kukulies, J., Senf, F., Marinescu, P. J., Heikenfeld, M., Brunner, K. N., Bruning, E. C., Collis, S. M., Jackson, R. C., Leung, G. R., Pfeifer, N., Raut, B. A., Saleeby, S. M., Stier, P., & Van Den Heever, S. C. (2024). tobac v1.5: introducing fast 3D tracking, splits and mergers, and other enhancements for identifying and analysing meteorological phenomena. Geoscientific Model Development, 17(13), 5309–5330. https://doi.org/10.5194/gmd-17-5309-2024

Stanković, A., Messori, G., Pinto, J. G., & Caballero, R. (2024). Large-scale perspective on extreme near-surface winds in the central North Atlantic. Weather and Climate Dynamics, 5(2), 821–837. https://doi.org/10.5194/wcd-5-821-2024

Stewart, S. R. (2018). Tropical Cyclone Report: Hurricane Ophelia, 9 - 15 October 2017. https://www.nhc.noaa.gov/data/tcr/AL172017_Ophelia.pdf

https://doi.org/10.5194/egusphere-2026-2701
Preprint. Discussion started: 22 May 2026

Sugi, M., Noda, A., & Sato, N. (2002). Influence of the Global Warming on Tropical Cyclone Climatology: An Experiment with the JMA Global Model. Journal of the Meteorological Society of Japan, 80(2), 249–272. https://doi.org/https://doi.org/10.2151/jmsj.80.249

The COMET Program. (2009). Tropical Cyclones. In Introduction to Tropical Meteorology, Version 1.3. (10). https://www.meteo.physik.uni-muenchen.de/~roger/Mtheory/Ch10_Tropical_Cyclones.pdf

The Saffir-Simpson Team, Schott, T., Landsea, C., Hafele, G., Lorens, J., Taylor, A., Thurm, H., Ward, B., Willis, M., & Zaleski, W. (2012). The Saffir-Simpson Hurricane Wind Scale.

Villarini, G., & Vecchi, G. A. (2013). Projected increases in North Atlantic tropical cyclone intensity from CMIP5 models. Journal of Climate, 26(10), 3231–3240. https://doi.org/10.1175/JCLI-D-12-00441.1

Wasko, C., Sharma, A., & Westra, S. (2016). Reduced spatial extent of extreme storms at higher temperatures. Geophysical Research Letters, 43(8), 4026–4032. https://doi.org/10.1002/2016GL068509

Wernli, H., & Schwierz, C. (2006). Surface Cyclones in the ERA-40 Dataset (1958–2001). Part I: Novel Identification Method and Global Climatology. Journal of the Atmospheric Sciences, 63(10), 2486–2507. https://doi.org/10.1175/JAS3766.1

Wood, K., Yanase, W., Beven, J., Camargo, S. J., Courtney, J. B., Fogarty, C., Fukuda, J., Kitabatake, N., Kucas, M., McTaggart-Cowan, R., Reboita, M. S., & Riboldi, J. (2023). Phase transitions between tropical, subtropical, and extratropical cyclones: A review from IWTC-10. Tropical Cyclone Research and Review, 12(4), 294–308. https://doi.org/10.1016/j.tcrr.2023.11.002

Yamada, Y., Satoh, M., Sugi, M., Kodama, C., Noda, A. T., Nakano, M., & Nasuno, T. (2017). Response of tropical cyclone activity and structure to global warming in a high-resolution global nonhydrostatic model. Journal of Climate, 30(23), 9703–9724. https://doi.org/10.1175/JCLI-D-17-0068.1

Zelinsky, D. A. (2019). Tropical Cyclone Report: Hurricane Lorenzo, 23 September - 2 October 2019. https://www.nhc.noaa.gov/data/tcr/AL132019_Lorenzo.pdf

Zhao, K., Zhao, H., Klotzbach, P. J., Wu, L., Wang, C., & Cao, J. (2026). Anthropogenic warming projected to drive a decline in global tropical cyclone frequency in CMIP6 simulations. Npj Climate and Atmospheric Science. https://doi.org/10.1038/s41612-026-01330-x